

Performance enhancement of ZnO nanowires/PbS quantum dot depleted bulk heterojunction solar cells with an ultrathin Al_2O_3 interlayer

Shuaipu Zang(臧帅普), Yinglin Wang(王莹琳), Meiying Li(李美莹), Wei Su(苏蔚), Meiqi An(安美琦), Xintong Zhang(张昕彤), Yichun Liu(刘益春)
Citation: Chin. Phys. B . 2018, 27(1): 018503. **doi:** 10.1088/1674-1056/27/1/018503

Journal homepage: http://cpb.iphy.ac.cn; http://iopscience.iop.org/cpb

What follows is a list of articles you may be interested in

Improved performance of Ge n^+/p diode by combining laser annealing and epitaxial Si passivation

Wang Chen(王尘), Xu Yihong(许怡红), Li Cheng(李成), Lin Haijun(林海军)
Chin. Phys. B . 2018, 27(1): 018502. **doi:** 10.1088/1674-1056/27/1/018502

Studies on the polycrystalline silicon/SiO_2 stack as front surface field for IBC solar cells by two-dimensional simulations

Shuai Jiang(姜帅), Rui Jia(贾锐), Ke Tao(陶科), Caixia Hou(侯彩霞), Hengchao Sun(孙恒超), Zhiyong Yu(于志泳), Yongtao Li(李勇滔)
Chin. Phys. B . 2017, 26(8): 087802. **doi:** 10.1088/1674-1056/26/8/087802

Direct observation of the carrier transport process in InGaN quantum wells with a pn-junction

Haiyan Wu(吴海燕), Ziguang Ma(马紫光), Yang Jiang(江洋), Lu Wang(王禄), Haojun Yang(杨浩军), Yangfeng Li(李阳锋), Peng Zuo(左朋), Haiqiang Jia(贾海强), Wenxin Wang(王文新), Junming Zhou(周钧铭), Wuming Liu(刘伍明), Hong Chen(陈弘)
Chin. Phys. B . 2016, 25(11): 117803. **doi:** 10.1088/1674-1056/25/11/117803

Enhancement of terahertz coupling efficiency by improved antenna design in GaN/AlGaN high electron mobility transistor detectors

Sun Yun-Fei, Sun Jan-Dong, Zhang Xiao-Yu, Qin Hua, Zhang Bao-Shun, Wu Dong-Min
Chin. Phys. B . 2012, 21(10): 108504. **doi:** 10.1088/1674-1056/21/10/108504

SPECIAL TOPIC — New generation solar cells

Performance enhancement of ZnO nanowires/PbS quantum dot depleted bulk heterojunction solar cells with an ultrathin Al_2O_3 interlayer*

Shuaipu Zang(臧帅普)[1,#], Yinglin Wang(王莹琳)[1,2,†], Meiying Li(李美莹)[1], Wei Su(苏蔚)[1], Meiqi An(安美琦)[1], Xintong Zhang(张昕彤)[1,2,‡], and Yichun Liu(刘益春)[1,2]

[1] *Center for Advanced Optoelectronic Materials Research, School of Physics, and Key Laboratory of UV-Emitting Materials and Technology of Chinese Ministry of Education, Northeast Normal University, Changchun* 130024, *China*

[2] *National Demonstration Center for Experimental Physics Education, Northeast Normal University, Changchun* 130024, *China*

(Received 29 September 2017; revised manuscript received 29 November 2017; published online 13 December 2017)

Depleted bulk heterojunction (DBH) PbS quantum dot solar cells (QDSCs), appearing with boosted short-circuit current density (J_{sc}), represent the great potential of solar radiation utilization, but suffer from the problem of increased interfacial charge recombination and reduced open-circuit voltage (V_{oc}). Herein, we report that an insertion of ultrathin Al_2O_3 layer (ca. 1.2 Å thickness) at the interface of ZnO nanowires (NWs) and PbS quantum dots (QDs) could remarkably improve the performance of DBH-QDSCs fabricated from them, i.e., an increase of V_{oc} from 449 mV to 572 mV, J_{sc} from 21.90 mA/cm^2 to 23.98 mA/cm^2, and power conversion efficiency (PCE) from 4.29% to 6.11%. Such an improvement of device performance is ascribed to the significant reduction of the interfacial charge recombination rate, as evidenced by the light intensity dependence on J_{sc} and V_{oc}, the prolonged electron lifetime, the lowered trap density, and the enlarged recombination activation energy. The present research therefore provides an effective interfacial engineering means to improving the overall performance of DBH-QDSCs, which might also be effective to other types of optoelectronic devices with large interface area.

Keywords: interface charge recombination, Al_2O_3 interlayer, passivation, PbS quantum dots

PACS: 85.35.Be, 78.67.Lt, 73.63.Kv, 62.23.Hj **DOI:** 10.1088/1674-1056/27/1/018503

1. Introduction

Due to their unique characteristics, colloidal quantum dots have attracted extensive interests from both fundamental and applied points of view.[1–5] During the last decade, a new type of solar cells with PbS QDs layer as absorber was developed rapidly and showed many advantages towards future photovoltaics, such as tailored light-harvesting, solution-based deposition technology, and good air stability.[6–10] However, the compromise of light absorption and carrier collection still serves as a big obstacle towards its further improvement.[11] The depleted bulk heterojunction (DBH) structure was proved to deal with the compromise skillfully through orthogonalization of the directions of light absorption and carrier collection.[12] The short-circuit current density of quantum dot solar cells (QDSCs) with DBH structure was boosted strikingly, while the power conversion efficiency was increased insufficiently because of the reduced open-circuit voltage caused by the increased interface charge recombination.[12,13]

Interface charge recombination can usually be reduced through interface engineering, such as interface energy level alignment and interface passivation.[14–19] In PbS QDSCs, MgZnO buffer layer and dipolar molecule were proved to elevate the interface energy level of ZnO and then increase the open-circuit voltage (V_{oc}).[14,15] Nevertheless, the elevated ZnO energy level is not beneficial to photoelectron injection from PbS QDs, thus it is harmful to the short-circuit current density (J_{sc}) in principle. Depositing an insulating layer at the ZnO NWs/PbS QDs interface was another effective strategy to reduce the recombination. Ultrathin $Mg(OH)_2$ interlayer was proved to successfully suppress the interface charge recombination through effects of interface passivation and tunneling barrier as discussed in our previous report.[17] But the overlarge barrier width was blamed for the decreased J_{sc}. Therefore, an optimal interface modification strategy is in urgent need to solve interface charge recombination and improve J_{sc} synchronously.

Herein, we utilized a modified sol–gel process to prepare an ultrathin Al_2O_3 interlayer at the ZnO NWs/PbS QDs interface using the aluminum sec-butoxide as the precursor. With this Al_2O_3 interlayer, the interface charge recombina-

*Project supported by the National Natural Science Foundation of China (Grant Nos. 91233204, 51372036, and 51602047), the Key Project of Chinese Ministry of Education (Grant No. 113020A), and the 111 Project, China (Grant No. B13013).

#Present address: School of Physics & Electrical Engineering, Anyang Normal University.

†Corresponding author. E-mail: wangyl100@nenu.edu.cn

‡Corresponding author. E-mail: xtzhang@nenu.edu.cn

© 2018 Chinese Physical Society and IOP Publishing Ltd

tion was distinctly reduced as successively confirmed by light intensity dependence on V_{oc} and J_{sc} and prolonged electron lifetime. From the temperature dependence on V_{oc}, the recombination activation energy was increased from 0.55 eV to 0.96 eV, which suggests that the V_{oc} was less limited by Fermi level pinning after depositing the Al_2O_3 interlayer. Further, a calculation of density of states also confirmed that the trap density was reduced in devices with the Al_2O_3 interlayer. This reduced trap density was further elucidated from photoluminescence measurements, where the luminescence associated with the ZnO surface defects at 500–600 nm was significantly decreased with the ca. 1.2 Å-thick Al_2O_3 interlayer. These improvements led to an enhancement of the device performance, which had an increase of V_{oc} from 449 mV to 572 mV, J_{sc} from 21.90 mA/cm^2 to 23.98 mA/cm^2, and power conversion efficiency (PCE) from 4.29% to 6.11%.

2. Methods

2.1. Materials

Zinc acetate dehydrate (99%), zinc nitrate hexahydrate (99%), and lead oxide (99%) were purchased from Beijing Chemical Reagent Co. 1,2-ethanedithiol (EDT, 97%), ethylene imine polymer (PEI, MW = 600, 99%), aluminum sec-butoxide (97%), isopropanol (99.9%), hexamethylenetetramin (HMTA, 99%), and acetonitrile (99%) were purchased from Aladdin. Tetrabutylammonium iodide (TBAI, 98%), oleic acid (OA, 99%), hexamethyldisilathiane (TMS, 99%), and 1-octadecene (ODE, 90%) were purchased from Aldrich. All chemicals were used as received without purification. SnO_2:F (FTO) conductive substrates (15 Ω/sq) were purchased from Nippon Sheet Glass.

2.2. Solar cell fabrication

PbS QDs with a bandgap of 1.50 eV were synthesized according to the previous literature.[20] FTO substrates were cleaned as in our previous report.[21] ZnO nanowires array with a length of ∼ 600 nm was obtained through solvent thermal process.[22] Aluminum sec-butoxide was diluted in isopropanol (1:5000; V:V) to prepare the precursor solution. It should be noted that this process must be taken in inert atmosphere because of the extreme sensitivity of aluminum sec-butoxide to moisture. But the diluted solution remains stable in air for hours. The Al_2O_3 interlayer was prepared from this precursor solution by spin-coating in air, following by annealing at 80 °C for 30 min in air. And the ZnO nanowires substrates for cells without Al_2O_3 interlayer also underwent the same annealing process before PbS QDs deposition. PbS QDs were deposited with a ligand exchange process according to the previous report.[23] Au electrode was finished after thermal evaporation. The area of single cell was 0.053 cm^2. All cells were stored and tested in air condition.

2.3. Characterization

The cross-sectional morphology of the cell was observed with an FEI Quanta 250 scanning electron microscope (SEM). The x-ray photoelectron spectra were measured with an ESCALAB 250 spectrometer equipped with a hemispherical electron energy analyzer using the Al $K\alpha$ radiation ($h\nu$ = 1486.6 eV) and an energy step of 0.1 eV. The electron take-off angle was 90°. The photoelectron spectra were recorded in constant analyzer energy mode. Photoluminescence measurement was conducted on a J-Y Horiba UVlamb micro-Raman spectrometer in a back-scattering configuration, using a 325 nm He–Cd laser for excitation. Current density–voltage (J–V) characteristics were recorded on a Keithley 2400 A source meter under AM 1.5 G irradiation supplied by a Sun 2000 solar simulator (ABET Technology). Open-circuit photovoltage decay and charge extraction were carried out with a Modulab XM PhotoEchem station (Solartron Analytical) and a 680 nm diode light (M680L4 Thorlabs) as the excitation source. All measurements were performed in air. The cells were stored in ambient air between measurements without encapsulation.

3. Results and discussion

Previously, we reported that a solution-deposited $Mg(OH)_2$ interlayer could effectively reduce the interface charge recombination and increase V_{oc} in DBH PbS QDSCs.[17] However, the barrier width still brought a decrease in J_{sc} even under the optimum condition of interlayer (15.5 Å). Therefore, a more suitable insulating interlayer is needed to improve the cell performance. As aluminum sec-butoxide has a larger volume shrinkage than magnesium methoxide after hydrolysis in air, a smaller barrier width could be obtained accompanying with a thinner interlayer, and the goal of improving V_{oc} and J_{sc} synchronously may be accomplished.

DBH PbS QDSCs with Al_2O_3 interlayer were then fabricated to verify our conjecture. All cells were stored and measured under atmospheric condition. Figure 1(a) shows the schematic diagram of the cells with DBH structure, which was proved to promote photocurrent on the sacrifice of photovoltage owing to the increased interface charge recombination.[12] A solution prepared Al_2O_3 interlayer was added at the ZnO NWs/PbS QDs interface, aiming at reducing the interface charge recombination. Figure 1(b) shows the cross-sectional morphology of the cell, where PbS QDs are fully filled in ZnO NWs, and the part of the PbS QDs layer beyond the ZnO NWs is needed to avoid short circuit formed by direct contact of Au and ZnO NWs.

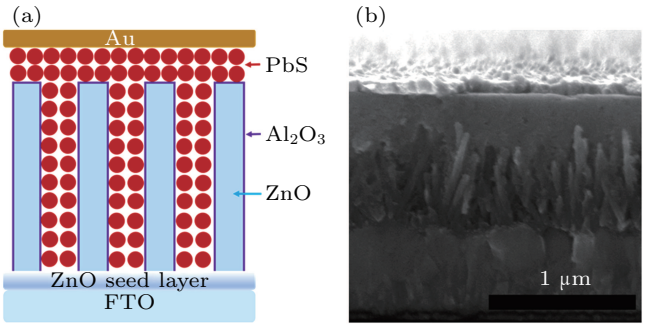


Fig. 1. (color online) (a) Schematic diagram of cells with FTO/ZnO NWs/PbS/Au DBH structure; (b) cross-sectional SEM image of the cell.

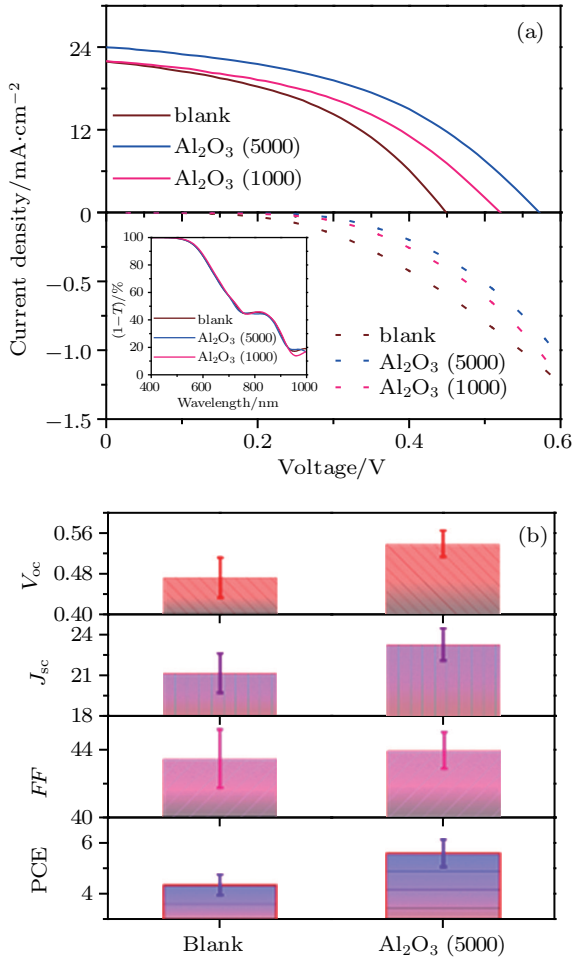


Fig. 2. (color online) (a) J–V characteristics of cells with and without Al_2O_3 interlayer under dark and AM 1.5 G solar irradiation (100 mW/cm^2), and cells transmittance data were shown in the insert; (b) parameters statistics for 5 cells with and without Al_2O_3 interlayer.

Photocurrent density–voltage (J–V) characteristics were measured under AM 1.5 G solar irradiation (100 mW/cm^2). In Fig. 2(a), the cells with Al_2O_3 interlayer present an extremely prominent increase of V_{oc} from 449 mV to 572 mV (Table 1). This huge V_{oc} promotion is mainly attributed to the reduced charge recombination from PbS QDs light absorbing layer to ZnO electron transport layer.[16] What is more, the J_{sc} increases from 21.90 mA/cm^2 to 23.98 mA/cm^2 (Table 1) after excluding the effect of light absorption (insert in Fig. 1(a)), leading to a final increase of PCE from 4.29% to 6.11% (Table 1). We also optimized the thickness of the Al_2O_3 interlayer by controlling the dilution ratio of aluminum sec-butoxide. When the dilution ratio is less than 1000, the diluted solution could not be stable in air. In the case of dilution ratio greater than 5000, the consistency of cells performance becomes terrible, which may be caused by the nonuniformity of the formed Al_2O_3 interlayer. And the cells performance achieves the best when the dilution ratio is equal to 5000. Statistics results in Fig. 2(b) further confirm the full improvement of the cells performance with Al_2O_3 interlayer. These results are completely consistent with our conjecture.

Table 1. Parameters of the cells.

Cells	V_{oc}/mV	J_{sc}/mA·cm^{-2}	FF/%	PCE/%
Blank	473 ± 38	21.24 ± 1.40	43.46 ± 1.66	4.36 ± 0.39
Al_2O_3 (1000)	501 ± 14	21.94 ± 0.16	44.25 ± 0.33	4.87 ± 0.13
Al_2O_3 (5000)	543 ± 25	23.28 ± 1.15	44.00 ± 1.04	5.59 ± 0.53
Champion	572	23.98	44.54	6.11

Series of measurements were then conducted to investigate the effect of the Al_2O_3 interlayer on the performance of cells. Light intensity dependence of J_{sc} and V_{oc} was firstly observed. The J_{sc} highly depends on the light intensity and can be expressed as $J_{sc} \propto I^{\alpha}$, where I and α are the light intensity and the exponential factor, respectively.[24–26] $\alpha = 1$ means that the absorbed photon converts into electron equivalently, and the recombination during the charge carrier collection is not dependent on the light intensity. In Fig. 3(a), α values of 0.924 and 0.942 are calculated for the cells without and with Al_2O_3 interlayer, which indicates that the charge recombination is reduced under the short-circuit condition.

The diode ideality factor n is an indicator of the dominant recombination mechanism, which can be deduced from $J_{sc} \propto I^{\alpha}$ and

$$V_{oc} = \frac{nkT}{q} \ln\left(\frac{J_{sc}}{J_0}\right), \tag{1}$$

where k, T, q, and J_0 are the Boltzmann constant, the temperature in Kelvin, the elementary charge, and the reverse saturation current density, respectively. The ideality factor $n = 1$ means that the band to band recombination is dominant, and when the trap-assisted recombination dominates, $n = 2$.[27] In Fig. 3(b), the cell with Al_2O_3 interlayer exhibits a different light intensity dependence of V_{oc} with $n = 1.63$, whereas in the cell without Al_2O_3 interlayer, $n = 1.82$. The light intensity dependences of J_{sc} and V_{oc} for the two cells therefore suggest that there is a higher interface trap-assisted recombination in the cell without Al_2O_3 interlayer. These results manifest that the Al_2O_3 interlayer reduces the density of interfacial traps and improves the charge extraction.

The temperature dependence of V_{oc} in Fig. 3(c) could give an insight into the carrier generation-recombination processes. The activation energy E_a can be deduced from Fig. 3(c) according to [27]

$$V_{oc} = \frac{E_a}{q} - \frac{nkT}{q} \ln\left(\frac{J_{00}}{J_{sc}}\right), \tag{2}$$

where J_{00} is the prefactor. In the high temperature region, n, J_{00}, and J_{sc} are nearly temperature-independent, and E_a can be obtained by extrapolating V_{oc} to 0 K. In Fig. 3(c), E_a of the cell increases from 0.55 eV to 0.96 eV with the incorporation of the Al_2O_3 interlayer. This indicates that the V_{oc} is less limited by Fermi level pinning to the trap states after inserting the Al_2O_3 interlayer.[28] And we believe that the Al_2O_3 interlayer may passivate the trap states in ZnO, thus reducing the interface charge recombination.

Electron lifetime (τ_n) can also represent the rate of charge recombination from PbS to ZnO, and the larger τ_n the higher V_{oc}. To further make clear the origin of V_{oc} increase, open-circuit voltage decay (OCVD) measurements were carried out with a 680 nm diode light as the excitation source. Electron lifetime could be calculated from the cell open-circuit photovoltage decay behavior according to[29]

$$\tau_n = -\frac{k_B T}{e}\left(\frac{dV_{oc}}{dt}\right)^{-1}, \tag{3}$$

where k_B is the Boltzmann constant, T is the temperature, and e is the elementary charge. In Fig. 3(d), the longer τ_n at the same V_{oc} means a slower charge recombination rate of the cells with Al_2O_3 interlayer. This result agrees well with the cells J–V characteristics and results in Figs. 3(a)–3(c).

In order to gain more insight into the charge recombination, the trap density of the cells was investigated using charge extraction method. This measurement typically starts at open-circuit conditions under illumination. At time $t = 0$, the cell is switched to short-circuit with illumination turned off, the trapped electrons are then extracted and the number can be calculated by integrating current and time. The density of states (DOS) can be deduced from the number of trapped electrons. Since V_{oc} changes with the intensity of illumination, DOS in the cells can be estimated as a function of V_{oc}, as shown in Fig. 3(e). With the incorporation of the Al_2O_3 interlayer, the DOS exhibits a significant lower value. This result further positively demonstrates the effect of the Al_2O_3 interlayer on eliminating the trap density, suppressing the interface charge recombination, and improving the cell performance.

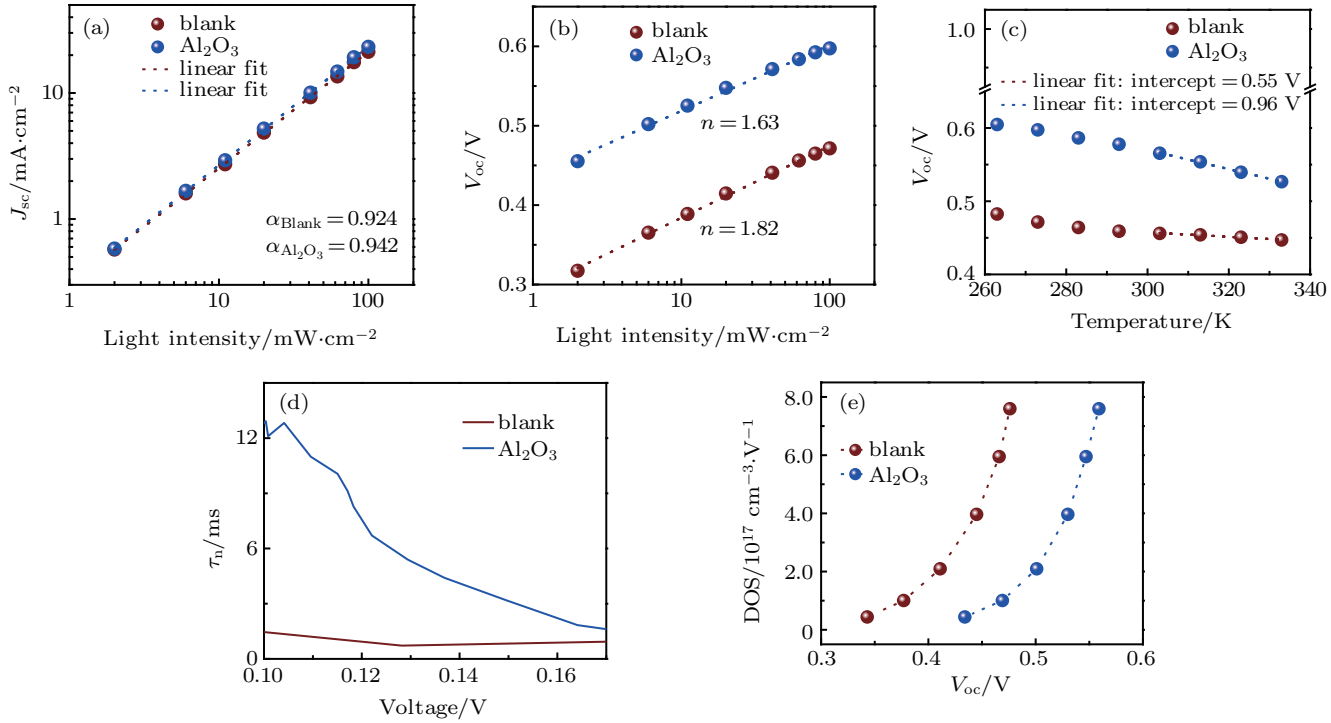


Fig. 3. (color online) Light intensity dependence of (a) J_{sc} and (b) V_{oc}; (c) activation energy calculation from temperature dependence of V_{oc} with light intensity of 100 mW/cm^2; (d) different electron lifetime of two cells inferred from their open-circuit photovoltage decay behavior; (e) density of states of two cells calculated from charge extraction measurements.

The obtained results demonstrate the significant promotion of the Al_2O_3 interlayer to V_{oc}. The highly reduced interface charge recombination ought to protect photoelectrons from trapping, thus increase J_{sc} at the same time, just as observed from the J–V characteristics of the cells with Al_2O_3 interlayer. But the previously reported $Mg(OH)_2$ interlayer showed harm to J_{sc}. We consider that the different barrier width, namely, the interlayer thickness, might be the origin of

this difference. Therefore, x-ray photoelectron spectroscopy (XPS) was utilized to estimate the thickness of the Al_2O_3 interlayer. Figure 4(a) shows the Zn $2p_{3/2}$ (1021.7 eV), O 1s (531.6 eV), and Al 2p (74.7 eV) signals variation without and with Al_2O_3 layer. The intensities of Zn $2p_{3/2}$ and O 1s attenuate obviously due to the blocking effect of the Al_2O_3 layer, which is shown in the inset of Fig. 4(a). And no new Zn $2p_{3/2}$ and O 1s peak are found after coating, which implies no other interaction occurred between ZnO NWs and the Al_2O_3 layer. The relatively weak but distinct peak appearing at 74.7 eV indicates the existence of the Al_2O_3 interlayer. The thickness of the Al_2O_3 interlayer is further estimated by using a two-layer model,[30] and 1.2 Å is calculated for the Al_2O_3 interlayer thickness. This thickness is dramatically decreased compared with the optimal thickness of the $Mg(OH)_2$ interlayer (15.5 Å). The huge volume shrinkage of aluminum sec-butoxide after hydrolysis is the main reason of this sharply decreased interlayer thickness.

In order to seek the reason of trap density reducing as analyzed above, room temperature photoluminescence measurements were conducted as shown in Fig. 4(b). The completely overlapped curves of UV emission at 377 nm suggest no band shift of ZnO occurred. And surface defects luminescence at 500–600 nm, generated from the oxygen vacancies, is obviously attenuated with the incorporation of the ultrathin Al_2O_3 interlayer, indicating the prominent passivation effect. This result demonstrates well the reason of trap density reduction and interface charge recombination decrease. And it also helps reducing trapped photoelectrons and increasing J_{sc} at the same time. Therefore, V_{oc} and J_{sc} have been improved simultaneously.

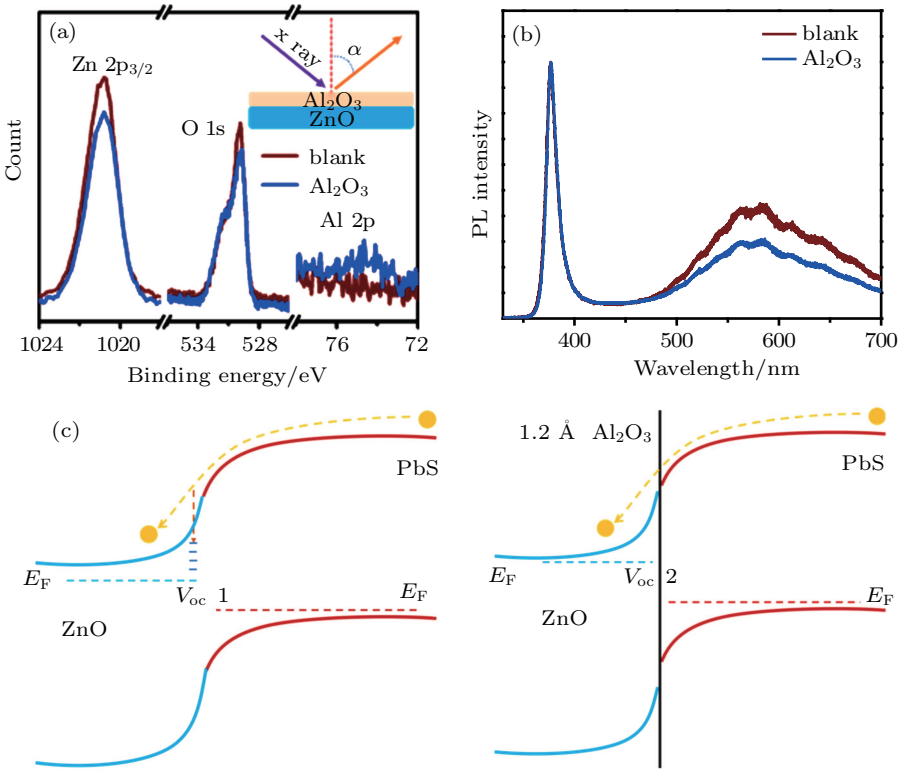


Fig. 4. (color online) (a) XPS spectra of Zn $2p_{3/2}$, O 1s, and Al 2p signals of ZnO NWs with and without aluminum sec-butoxide solution treatment; (b) comparison of PL characters of different ZnO NWs on FTO substrates (λ_{ex}: 325 nm), and the broad peak range from 500 nm to 650 nm results from the luminescence of surface defects of ZnO; (c) schematic illustration of effect of ultrathin Al_2O_3 interlayer on DBH PbS QDSCs.

4. Conclusion

In summary, we utilized the sol–gel process to prepare a 1.2 Å-thick Al_2O_3 interlayer at the ZnO NWs/PbS QDs interface in DBH PbS QDSCs. Obvious passivation effect was observed from photoluminescence measurements. Drastically reduced interface charge recombination was inferred from the light intensity dependence of V_{oc} and J_{sc}, and open-circuit decay measurements. Sharply increased recombination activation energy and reduced DOS also indicated reduced trap density in cells with Al_2O_3 interlayer. Therefore, V_{oc}, J_{sc}, and PCE of the cells were improved simultaneously. This work may enlighten other type of cells in dealing with such carrier recombination issues.

Acknowledgement

We highly appreciate the help of Dr. Hancheng Zhu, Lei Wang, and Jinhuan Li on material characterization and device measurements.

References

[1] Zarei H and Mekfar R 2015 *Chin. Phys. B* **25** 027103
[2] Deng M T, Vaitiekenas S, Hansen E B, Danon J, Leijnse M, Flensberg K, Krogstrup P, Marcus C M, Nygard J and Majorana 2016 *Science* **354** 1557
[3] Wei H, Wang G, Wu H, Luo Y, Li D and Meng Q 2016 *Acta Phys. Chim. Sin.* **32** 201
[4] An X T 2014 *Chin. Phys. B* **23** 107301
[5] Yan F L, Zhang J C, Yao D Y, Liu F Q, Wang L J, Liu J Q and Wang Z G 2015 *Chin. Phys. B* **24** 024212
[6] Yuan M, Liu M and Sargent E H 2016 *Nat. Energy* **1** 1
[7] Lan X, Voznyy O, Kiani A, Arquer F P G D, Abbas A S, Kim G, Liu M, Yang Z, Walters G, Xu J, Yuan M, Ning Z, Fan F, Kanjanaboos P, Kramer I, Zhitomirsky D, Lee P, Perelgut A, Hoogland S and Sargent E H 2016 *Adv. Mater.* **28** 299
[8] Ip A H, Thon S M, Hoogland S, Voznyy O, Zhitomirsky D, Debnath R, Levina L, Rollny L R, Carey G H, Fischer A, Kemp K W, Kramer I J, Ning Z, Labelle A J, Chou K W, Amassian A and Sargent E H 2012 *Nat. Nanotech.* **7** 577
[9] Wang H, Pedro V G, Kubo T, -Santiago F F, Bisquert J, Sanehira Y, Nakazaki J and Segawa H 2015 *J. Phys. Chem. C* **119** 27265
[10] Wang Y, Su W, Zang S, Li M, Zhang X and Liu Y 2017 *Appl. Phys. Lett.* **110** 163902
[11] Zhitomirsky D, Voznyy O, Hoogland S and Sargent E H 2013 *ACS Nano* **7** 5282
[12] Barkhouse D A R, Debnath R, Kramer I J, Zhitomirsky D, -Abraham A G P, Levina L, Etgar L, Grätzel M and Sargent E H 2011 *Adv. Mater.* **23** 3134
[13] Wang H, Kubo T, Nakazaki J, Kinoshita T and Segawa H 2013 *J. Phys. Chem. Lett.* **4** 2455
[14] Kim G, Arquer F P G D, Yoon Y, Lan X, Liu M, Voznyy O, Yang Z, Fan F, Ip A H, Kanjanaboos P, Hoogland S, Kim J Y and Sargent E H 2015 *Nano Lett.* **15** 7691
[15] Zhang X and Johansson E M 2017 *J. Mater. Chem. A* **5** 303
[16] Chang J, Kuga Y, Mora-Sero I, Toyoda T, Ogomi Y, Hayase S, Bisquert J and Shen Q 2015 *Nanoscale* **7** 5446
[17] Zang S, Wang Y, Su W, Zhu H, Li G, Zhang X and Liu Y 2016 *Phys. Status Solidi* **10** 745
[18] Dong J, Zhao Y, Shi J, Wei H, Xiao J, Xu X, Luo J, Xu J, Li D, Luo Y, Meng Q 2014 *Chem. Commun.* **50** 13381
[19] Bashiri H, Karami M A and Mohammadnejad S 2017 *Chin. Phys. B* **26** 108801
[20] Hines M A and Scholes G D 2003 *Adv. Mater.* **15** 1844
[21] Zang S, Wang Y, Li M, Su W, Zhu H, Zhang X and Liu Y 2017 *Sol. Energy Mater. Sol. Cells* **169** 264
[22] Xu C, Shin P, Cao L and Gao D 2010 *J. Phys. Chem. C* **114** 125
[23] Chuang C H M, Brown P R, Bulović V and Bawendi M G 2014 *Nat. Mater.* **13** 796
[24] Kyaw A K, Wang D H, Wynands D, Zhang J, Nguyen T Q, Bazan G C and Heeger A J 2013 *Nano Lett.* **13** 3796
[25] Riedel I, Parisi J, Dyakonov V, Lutsen L, Vanderzande D and Hummelen J C 2004 *Adv. Funct. Mater.* **14** 38
[26] van Duren J K J, X. N. Yang X N, Loos J, Bulle-Lieuwma C W T, Sieval A B, Hummelen J C and Janssen R A J 2004 *2004 Adv. Funct. Mater.* **14** 425
[27] Chuang C M, Maurano A, Brandt R E, Hwang G W, Jean J, Buonassisi T, Bulovic V and Bawendi M G 2015 *Nano Lett.* **15** 3286
[28] Rath A, Pelayo Garcia de Arquer F, Stavrinadis A, Lasanta T, Bernechea M, Diedenhofen S L and Konstantatos G 2014 *Adv. Mater.* **26** 4741
[29] Zaban A, Greenshtein M and Bisquert J 2003 *Chem. Phys. Chem.* **4** 859
[30] Hochella M F and Carim A H 1988 *Surf. Sci.* **197** L260